Bol. Soc. Paran. Mat.
©SPM – E-ISSN-2175-1188
SPM: www.spm.uem.br/bspm

(3s.) **v. 2025 (43)** : 1–16.
ISSN-0037-8712
doi:10.5269/bspm.77951

# Using two-dimensional Bernstein polynomials to simulate two-dimensional linear stochastic fredholm integral equations with multiple noise source

Murtadha Ali Shabeeb, Mohsen Fallahpour, Reza Ezzati and Mohammad Navaz Rasoulizadeh

ABSTRACT: This paper presents a numerical method based on two-dimensional Bernstein polynomials (2DBPs) for the efficient solution of systems of two-dimensional linear multi-noise stochastic Fredholm integral equations (2D-LMN-SFIEs). The proposed approach is theoretically supported by a set of convergence theorems that also underline its distinctive advantages. Its effectiveness is demonstrated through two illustrative examples, which showcase the method's high accuracy and practical applicability. The obtained results demonstrate the robustness of the proposed approach in addressing complex stochastic integral equations, thereby affirming its significance for both theoretical investigations and practical problem-solving in applied mathematics.

Key Words: Two-dimensional stochastic integral, Fredholm integral equation, Bernstein polynomials, Brownian motion process, multiple noise, operational matrix.

## Contents



## 1. Introduction

The study of integral equations constitutes a cornerstone of applied mathematics, with a broad spectrum of applications spanning physics, engineering, and economics. Among the different classes of integral equations, the Fredholm type occupies a prominent role owing to its capability to model systems with fixed integration limits [1,2,3,4,5]. The complexity of such equations increases substantially when extended to higher-dimensional domains and when stochastic components are incorporated. Moreover, integral equations are indispensable in the formulation, theoretical analysis, and numerical solution of fractional differential equations, as numerous fractional operators can be equivalently represented through integrals with memory-dependent kernels [6,7,8,9,10]. This representation effectively captures the inherent nonlocality of fractional models and underpins their widespread applicability in modeling complex dynamical systems [11,12,13,14,15].

2010 *Mathematics Subject Classification:* 65C20, 60H20, 45A05, 14F10, 45B05, 90B50, 65L20.
Submitted July 19, 2025. Published September 01, 2025

In this paper, we examine a two-dimensional linear multi-noise stochastic Fredholm integral equation (2D-LMN-SFIE) of the second kind:

$$h(u,v) = q(u,v) + \int_0^1 \int_0^1 K_1(u,v,\eta,\mu)h(\eta,\mu)\,d\eta\,d\mu + \sum_{j=1}^{N} \int_0^1 \int_0^1 K_2(u,v,\eta,\mu)h(\eta,\mu)\,d\mathcal{B}_j(\eta)\,d\mathcal{B}_j(\mu), \tag{1.1}$$

where $(u,v) \in [0,1]^2$ and $(u,v,\eta,\mu) \in [0,1]^4$ with the condition $\eta \leqslant u < \mu \leqslant v$. The functions $q(u,v)$, $K_1(u,v,\eta,\mu)$, and $K_2(u,v,\eta,\mu)$ in the 2D-LMN-SFIE (1.1) are known, while $h(u,v)$ is the unknown function. Additionally, $\mathcal{B}(u) = (\mathcal{B}_1(u), \mathcal{B}_2(u), \ldots, \mathcal{B}_m(u))$ represents a multidimensional Brownian motion process, and the term $\int_0^1 \int_0^1 K_2(u,v,\eta,\mu)h(\eta,\mu)\,d\mathcal{B}_j(\eta)\,d\mathcal{B}_j(\mu)$ for $j = 1, 2, \ldots, N$ demonstrates the double Wiener-Itô integral.

In recent years, various numerical methods have been developed for solving stochastic integral equations. Fallahpour and his co-workers [16,17,18] employed techniques based on block-pulse functions (BPFs) and Haar wavelet functions (HWFs) for approximating two-dimensional linear stochastic integral problems. Mirzaee et al. [19] introduced a straightforward numerical approach combining two-dimensional moving least squares (2D-MLS) with the spectral-collocation technique for approximating two-dimensional stochastic Itô–Volterra integral equations. Singh and Saha Ray [20] presented a dependable numerical method for solving $n$-dimensional stochastic Itô–Volterra integral equations by applying the properties of Genocchi polynomials and introducing an operational matrix to transform the integral equation into an algebraic equation. Boukhelkhal and Zeghdane [21] proposed a robust computational method based on the Lagrange basis and Jacobi–Gauss collocation for approximating a class of nonlinear stochastic Itô–Volterra integral equations. Amin et al. [22] applied the shifted Jacobi–Gauss collocation technique to simulate mixed Volterra–Fredholm integral equations by reducing them to a system of algebraic equations that are easily solvable. Mi and Huang [23] introduced a technique for solving two-dimensional nonlinear Volterra–Fredholm integral equations with Lagrange interpolation and Legendre–Gauss quadrature.

Given the complexity of the 2D-LMN-SFIE, it is crucial to develop efficient efficient and accurate numerical methods. These methods aim to provide approximate solutions that are computationally feasible while maintaining a high degree of accuracy. The challenge lies in handling the dual aspects of the problem: the two-dimensional nature of the equation and the presence of multiple stochastic noise components. Traditional methods often fall short in addressing these challenges simultaneously, necessitating the development of more sophisticated approaches. Bernstein polynomials (BPs) hold significant importance in various mathematical fields and have been extensively applied to solve integral equations and in approximation theory [26,29]. Shekarabi et al. [29] introduced operational matrices for 2DBPs to address 2D ordinary Volterra-Fredholm integral problems.

In this study, we develop an efficient and conceptually straightforward computational framework for the numerical approximation of solutions to the two-dimensional linear multi-noise stochastic Fredholm integral equation (2D-LMN-SFIE) (1.1). The proposed approach is founded on the construction of two-dimensional Bernstein polynomials (2DBPs) over the unit square $[0,1]^2$, leveraging their favorable approximation properties to attain high numerical accuracy. By expanding both the unknown solution and the associated integral operators in terms of Bernstein polynomial functions (BPFs), the original stochastic integral equation is systematically transformed into a finite system of algebraic equations. This reduction substantially alleviates the inherent analytical complexity of the problem, rendering it more tractable for computational implementation. A rigorous error analysis for the BPF-based approximation is provided to establish the theoretical reliability and convergence characteristics of the method. Moreover, a comparative performance evaluation with several conventional numerical schemes is conducted, illustrating the superior efficiency, stability, and robustness of the proposed formulation in solving the 2D-LMN-SFIE (1.1).

The remainder of this paper is organized as follows: Section 2 introduces the fundamental concepts and properties of the 2DBPs. Section 3 details the application of the proposed method to approximate the 2D-LMN-SFIE (1.1). Section 4 is devoted to a rigorous error analysis of the method. Section 5 presents a set of numerical experiments to demonstrate the convergence, accuracy, and effectiveness of

the approach, together with a comparative analysis against alternative numerical techniques. In this section, 95% confidence intervals are also constructed for each computed solution. Finally, Section 6 summarizes the main findings and outlines concluding remarks.

## 2. Basic concepts of the multivariate BPs

First, regarding the stochastic Fredholm double Wiener-Itô integral, we introduce the following theorem.

**Theorem 1** Consider $\psi(\mu,\eta) \in L^2([\alpha,\beta]^2)$. Then, we have

$$\int_\alpha^\beta \int_\alpha^\beta \psi(\mu,\eta) d\mathcal{B}(\mu) d\mathcal{B}(\eta) = 2\int_\alpha^\beta \left[\int_\alpha^\mu \hat{\psi}(\mu,\eta) d\mathcal{B}(\eta)\right] d\mathcal{B}(\mu),$$

where $\hat{\psi}$ is the symmetrized version of $\psi$, defined as follows:

$$\hat{\psi}(\mu,\eta) = \frac{1}{2}\left(\psi(\mu,\eta) + \psi(\eta,\mu)\right)$$

.

Consider $q$ as a real-valued, bounded function defined over the closed $m$-dimensional space $[0,1]^n$. Let us define $V = (v_1, v_2, \ldots, v_m)$, where $V \in [0,1]^n$. The multivariate Bernstein polynomials $\mathbb{B}r_m(q;V)$ for the function $q$ are defined as in [25].

$$\mathbb{B}r_m(q;V) = \sum_{\alpha_1=0}^{m_1} \cdots \sum_{\alpha_m=0}^{m_m} q \begin{pmatrix} n_1^{-1}\alpha_1 \\ n_2^{-1}\alpha_2 \\ \vdots \\ n_m^{-1}\alpha_m \end{pmatrix} \times \binom{m_1}{\alpha_1} \ldots \binom{m_m}{\alpha_m} v_1^{\alpha_1}(1-v_1)^{m_1-\alpha_1} \ldots v_m^{\alpha_m}(1-v_m)^{m_m-\alpha_m}. \tag{2.1}$$

Here, $m_j,\ j = 1,2,\ldots,n$ represent positive integers. The nodal points $v_1, v_2, \ldots, v_m$ in (2.1) represent probabilities for a multivariate binomial distribution, which is formed based on the product of $m$ independent binomial distributions. The multivariate BPs $\mathbb{B}r_m(q;V)$ associated with $P_m$, in which $m = \sum_{j=1}^{n} m_j$ represents the total degree of $\mathbb{B}r_m(q;V)$, and $P_m$ represents the space of polynomials $P(V)$ of degree at most $n$, for every $V \in [0,1]^n$.

In view of (2.1), we examine the BPs of degree $(m_1 + m_2)$ on the interval $[0,1]^2$ as follows:

$$\mathbb{B}r_{(\alpha,m_1)(\beta,m_2)}(\eta,\mu) = \binom{m_1}{\alpha}\binom{m_2}{\beta}\eta^\alpha(1-\eta)^{m_1-\alpha}\mu^\beta(1-\mu)^{m_2-\beta},$$

where $\alpha = 0,1,\ldots,m_1$ and $\beta = 0,1,\ldots,m_2$ such that $m_1$ and $m_2$ represent arbitrary positive integers, the set of 2DBPs can be represented as a $(m_1+1)(m_2+1)$-vector $\Gamma(\eta,\mu)$ for $(\eta,\mu) \in [0,1]^2$.

$$\Gamma(\eta,\mu) = [\mathbb{B}r_{(0,m_1)(0,m_2)}(\eta,\mu), \ldots, \mathbb{B}r_{(0,m_1)(m_2,m_2)}(\eta,\mu), \ldots]. \tag{2.2}$$

$$\Gamma(\eta,\mu) = [\mathbb{B}r_{(0,m_1)(0,m_2)}(\eta,\mu), \ldots, \mathbb{B}r_{(0,m_1)(m_2,m_2)}(\eta,\mu), \ldots, \mathbb{B}r_{(m_1,m_1)(0,m_2)}(\eta,\mu), \ldots, \mathbb{B}r_{(m_1,m_1)(m_2,m_2)}(\eta,\mu)]^T.$$

The Bernstein polynomial (BP) for a function $h(\eta,\mu)$, defined on the interval $[0,1] \times [0,1]$, can be expressed as follows:

$$(\mathbb{B}r_{(m_1,m_2)}h)(\eta,\mu) = \sum_{\alpha=0}^{m_1}\sum_{\beta=0}^{m_2} h\left(\frac{\alpha}{m_1}, \frac{\beta}{m_2}\right)\mathbb{B}r_{(\alpha,m_1)(\beta,m_2)}(\eta,\mu) = H^T\Gamma(\eta,\mu). \tag{2.3}$$

In (2.2), using the properties of the 2DBPs as discussed in [29], we obtain:

$$\mathbb{B}r_{(\alpha,m_1)(\beta,m_2)}(\eta,\mu) = \mathcal{W}_{\alpha,\beta}\Omega_{m_1,m_2}(\eta,\mu),$$

for $\alpha = 0, 1, \ldots, m_1$, $\beta = 0, 1, \ldots, m_2$, where

$$\Omega_{m_1,m_2}(\eta,\mu) = [1, \mu, \mu^2, \ldots, \mu^{m_2}, \eta, \eta\mu, \eta\mu^2, \ldots, \eta\mu^{m_2}, \ldots, \eta^{m_1}, \eta^{m_1}\mu, \eta^{m_1}\mu^2, \ldots, \eta^{m_1}\mu^{m_2}]^T,$$

and $\mathcal{W}_{\alpha,\beta}$ is described in [29]. Consequently, the 2DBPs vector $\Gamma(\eta,\mu)$ defined in Eq. (2.2) can be expressed as:

$$\Gamma(\eta,\mu) = \mathcal{W}\Omega_{m_1,m_2}(\eta,\mu), \tag{2.4}$$

where $\mathcal{W}$ is a $(m_1+1)(m_2+1) \times (m_1+1)(m_2+1)$ matrix such that

$$\mathcal{W} = \begin{pmatrix} \mathcal{W}_{0,0} \\ \mathcal{W}_{0,1} \\ \vdots \\ \mathcal{W}_{m_1,m_2} \end{pmatrix}. \tag{2.5}$$

Similarly four-variables function $q(u,v,\eta,\mu)$, on $[0,1]\times[0,1]\times[0,1]\times[0,1]$ may be simulated with respect to 2DBPs such as:

$$q(u,v,\eta,\mu) \simeq \Gamma(u,v)^T \Lambda \Gamma'(\eta,\mu),$$

where $\Gamma(u,v)$ and $\Gamma'(\eta,\mu)$ are 2DBPs vectors of dimension $(m_1+1)(m_2+1)$, and $\Lambda$ is the $(m_1+1)(m_2+1) \times (m_1+1)(m_2+1)$ 2DBPs coefficients matrix.
By considering arbitrary $(m_1+1)(m_2+1)$ vector $\mathcal{C}$, we have

$$\Gamma(u,v)\Gamma^T(u,v)\mathcal{C} \simeq \tilde{\mathcal{C}}^T\Gamma(u,v). \tag{2.6}$$

Here $\tilde{\mathcal{C}}$ is defined as

$$\tilde{\mathcal{C}} = \breve{\mathcal{C}}\mathcal{W}^T,$$

in which $\breve{\mathcal{C}}$ and $\mathcal{W}$ are described in [29] and in equation (2.5), respectively.

### 2.1. Ordinary operational matrix of integration with 1d-BPs

The collection of 1D-BPs can be represented as a $(m_1+1)$-dimensional vector $\Gamma(\eta)$:

$$\Gamma(\eta) = [\mathbb{B}r_{(0,m_1)}(\eta), \mathbb{B}r_{(1,m_1)}(\eta), \ldots, \mathbb{B}r_{(m_1,m_1)}(\eta)]^T, \tag{2.7}$$

so we can write

$$\Gamma(\eta) = \mathcal{A}\Omega_{m_1}(\eta),$$

where $\Omega_{m_1}(\eta) = [1, \eta, \ldots, \eta^{m_1}]^T$ and $\mathcal{A}$ is an $(m_1+1)\times(m_1+1)$ upper triangular matrix with

$$\mathcal{A}_{\alpha+1}\left[\overbrace{0,0,\ldots,0}^{\alpha\ times}, (-1)^0\binom{m_1}{\alpha}\binom{m_1-\alpha}{0}, \ldots, (-1)^{m_1-\alpha}\binom{m_1}{\alpha}\binom{m_1-\alpha}{m_1-\alpha}\right]. \tag{2.8}$$

Let

$$\int_0^1 \Gamma(\eta)d\eta = \int_0^1 \mathcal{A}\Omega(\eta)d\eta = \mathcal{A}\left[\int_0^1 d\eta, \int_0^1 \eta d\eta, \ldots, \int_0^1 \eta^{m_1}d\eta\right]^T.$$

Therefore, we get

$$\int_0^1 \Gamma(\eta)d\eta = \mathcal{D}_o\Gamma(u),$$

with

$$\mathcal{D}_{o,(m_1+1)\times(m_1+1)} = \mathcal{A}\mathcal{A}'\mathcal{A}'', \tag{2.9}$$

where

$$\mathcal{A}' = \begin{pmatrix} 1 & 0 & \ldots & 0 \\ 0 & \frac{1}{2} & \ldots & 0 \\ \vdots & \vdots & \ddots & \vdots \\ 0 & 0 & \cdots & \frac{1}{m_1+1} \end{pmatrix},$$

such that the matrix $\mathcal{A}''$ represents a $(m_1+1)\times(m_1+1)$ matrix where all the elements are equal to 1.

### 2.2. Ordinary operational matrix of integration with 2D-BPs

To compute the ordinary double Fredholm integral of $\Gamma(\eta,\mu)$ as defined in (2.2), we express it as follows:

$$\int_0^1\int_0^1 \Gamma(\eta,\mu)d\eta d\mu \simeq Q_o\Gamma(u,v) = [\mathcal{D}_o \otimes \mathcal{D}_o]\Gamma(u,v), \tag{2.10}$$

where $u,v \in [0,1]$, and $Q_o$ is the $(m_1+1)(m_2+1)\times(m_1+1)(m_2+1)$ ordinary operational matrix of integration for 2DBPs. The matrix $\mathcal{D}_o$ is defined in Eq. (2.7), and $\otimes$ represents the Kronecker product, meaning:

$$R \otimes M = (r_{ij}M).$$

### 2.3. Stochastic operational matrix based on 1D-BPs

Similarly, for the 1D stochastic case, we have:

$$\int_0^1 \Gamma(\eta)d\mathcal{B}(\eta) = \int_0^1 \mathcal{A}\Omega(\eta)d\mathcal{B}(\eta) = \mathcal{A}\left[\int_0^1 d\mathcal{B}(\eta), \int_0^1 \eta d\mathcal{B}(\eta), \ldots, \int_0^1 \eta^{m_1} d\mathcal{B}(\eta)\right]^T, \tag{2.11}$$

where $\Omega(\eta)$ and $\mathcal{A}$ are defined in Eqs. (2.7) and (2.8), respectively. We can write

$$\begin{pmatrix} \int_0^1 d\mathcal{B}(\eta) \\ \int_0^1 \eta d\mathcal{B}(\eta) \\ \vdots \\ \int_0^1 \eta^{m_1} d\mathcal{B}(\eta) \end{pmatrix} = \begin{pmatrix} \mathcal{B}(1) \\ \mathcal{B}(1) - \int_0^1 \mathcal{B}(\eta)d\eta \\ \vdots \\ \mathcal{B}(1) - m_1\int_0^1 \eta^{m_1-1}\mathcal{B}(\eta)d\eta \end{pmatrix} = S = (s_\alpha)_{(m_1+1)\times 1},$$

where $s_\alpha = \mathcal{B}(1) - \alpha\int_0^1 \eta^{\alpha-1}\mathcal{B}(\eta)\,d\eta$ for $\alpha = 0,1,\ldots,m_1$. By applying the composite trapezium rule, we obtain:

$$s_\alpha = \mathcal{B}(1) - \frac{\alpha}{4}\left(2(\frac{1}{2})^{\alpha-1}\mathcal{B}(\frac{1}{2}) + \mathcal{B}(1)\right) = (1-\frac{\alpha}{4})\mathcal{B}(1) - \frac{\alpha}{2^\alpha}\mathcal{B}(\frac{1}{2}).$$

By substituting these approximations into Eq. (2.9), we obtain the following:

$$\int_0^1 \Gamma(\eta)d\mathcal{B}(\eta) = \mathcal{D}_s\Gamma(u),$$

with

$$\mathcal{D}_{s,(m_1+1)\times(m_1+1)} = \mathcal{A}J\mathcal{A}'', \tag{2.12}$$

where

$$J = \begin{pmatrix} \mathcal{B}(1) & 0 & \ldots & 0 \\ 0 & \frac{3}{4}\mathcal{B}(1) - \frac{1}{2}\mathcal{B}(0.5) & \ldots & 0 \\ \vdots & \vdots & \ddots & \vdots \\ 0 & 0 & \ldots & (1-\frac{m_1}{4})\mathcal{B}(1) - \frac{m_1}{2^{m_1}}\mathcal{B}(0.5) \end{pmatrix}.$$

### 2.4. Stochastic operational matrix with 2DBPs

In a similar manner, the stochastic double Fredholm integral of $\Gamma(\eta,\mu)$ can be approximated as follows:

$$\int_0^1\int_0^\mu \Gamma(\eta,\mu)d\mathcal{B}(\eta)d\mathcal{B}(\mu) \simeq Q_s\Gamma(u,v) = [\mathcal{D}_s \otimes \mathcal{P}_s]\Gamma(u,v), \tag{2.13}$$

where $u,v \in [0,1]$ and $Q_s$ is the stochastic operational matrix of integration for 2DBPs, with dimensions $(m_1+1)(m_2+1)\times(m_1+1)(m_2+1)$. In this context, $\mathcal{D}_s$ and $\mathcal{P}_s$ denote the stochastic operational matrices for 1D-BPs, as specified in Eq. (2.10) and discussed in [26].

## 3. Numerical implementation

This section uses the 2DBPs to approximate Eq. (1.1). Initially, applying Theorem 1, we consider the following steps:

$$\dot{K}_2(u,v,\eta,\mu)h(\eta,\mu) = \frac{1}{2}\left\{K_2(u,v,\mu,\eta)h(\mu,\eta) + K_2(u,v,\eta,\mu)h(\eta,\mu)\right\}. \tag{3.1}$$

Then, we can write

$$q(u,v) = \Gamma^T(u,v)Q, \tag{3.2}$$

$$K_1(u,v,\eta,\mu) = \Gamma^T(u,v)\Lambda\Gamma(\eta,\mu), \tag{3.3}$$

$$\dot{K}_2(u,v,\eta,\mu) = \Gamma^T(u,v)\dot{\Lambda}\Gamma(\eta,\mu), \tag{3.4}$$

and

$$h(u,v) = \Gamma^T(u,v)\mathcal{H}, \tag{3.5}$$

In Eq. (2.13), $Q$ denotes a vector with dimension $(m_1+1)(m_2+1)\times 1$, corresponding to the established vector of BP coefficients. Similarly, in Eq. (3.1) and Eq. (3.2), $\Lambda$ and $\dot{\Lambda}$ are $(m_1+1)(m_2+1)\times(m_1+1)(m_2+1)$ matrices that are also known BP coefficient matrices. Additionally, $\mathcal{H}$ in Eq. (3.5) is the unknown vector of BP coefficients given as:

$$\mathcal{H} = [h_{0,0}(u,v),\ldots,h_{0,m_2}(u,v),\ldots,h_{1,m_2}(u,v),\ldots,h_{m_1,m_2}(u,v)]^T.$$

By using relations (2.4), (2.8), (3.1) and (3.3), we have

$$\begin{aligned}\int_0^1\int_0^1 K_1(u,v,\eta,\mu)h(\eta,\mu)\,d\eta\,d\mu &\simeq \int_0^1\int_0^1 \Gamma^T(u,v)\Lambda\Gamma(\eta,\mu)\Gamma^T(\eta,\mu)G\,d\eta\,d\mu\\ &= \Gamma^T(u,v)\Lambda\left(\int_0^1\int_0^1\Gamma(\eta,\mu)\Gamma^T(\eta,\mu)G\,d\eta\,d\mu\right)\\ &\simeq \Gamma^T(u,v)\Lambda\tilde{\mathcal{C}_1}^T\left(\int_0^1\int_0^1\Gamma(\eta,\mu)\,d\eta\,d\mu\right)\\ &= \Gamma^T(u,v)\Lambda\tilde{\mathcal{C}_1}^T Q_o\Gamma(u,v).\end{aligned} \tag{3.6}$$

Likewise, by applying Theorem 1, the stochastic double integral in the problem (1.1) is discretized, yielding the following expression:

$$\begin{aligned}&\sum_{j=1}^N\int_0^1\int_0^1 K_2(u,v,\eta,\mu)h(\eta,\mu)d\mathcal{B}_j(\eta)d\mathcal{B}_j(\mu)\\ &\qquad = \sum_{j=1}^N 2\int_0^1\left[\int_0^\mu \dot{K}_2(u,v,\eta,\mu)h(\eta,\mu)d\mathcal{B}_j(\eta)\right]d\mathcal{B}_j(\mu),\end{aligned}$$

Using Eqs. (3.2) and (3.3), we obtain the following results:

$$\sum_{j=1}^N\int_0^1\int_0^1 K_2(u,v,\eta,\mu)h(\eta,\mu)d\mathcal{B}_j(\eta)d\mathcal{B}_j(\mu) = 2\sum_{j=1}^N\int_0^1\left[\int_0^\mu \Gamma^T(u,v)\dot{\Lambda}\Gamma(\eta,\mu)\Gamma^T(\eta,\mu)Qd\mathcal{B}_j(\eta)\right]d\mathcal{B}_j(\mu)$$

$$\sum_{j=1}^N\int_0^1\int_0^1 K_2(u,v,\eta,\mu)h(\eta,\mu)d\mathcal{B}_j(\eta)d\mathcal{B}_j(\mu) = 2\Gamma^T(u,v)\dot{\Lambda}\sum_{j=1}^N\left[\int_0^1\int_0^\mu \Gamma(\eta,\mu)\Gamma^T(\eta,\mu)Qd\mathcal{B}_j(\eta)d\mathcal{B}_j(\mu)\right].$$

The operational matrices $\tilde{\mathcal{C}_2}$ from (2.4) and $Q_s$ from (2.11) lead to the following conclusion:

$$\sum_{j=1}^N\int_0^1\int_0^1 K_2(u,v,\eta,\mu)h(\eta,\mu)d\mathcal{B}_j(\eta)d\mathcal{B}_j(\mu) = 2\Gamma^T(u,v)\dot{\Lambda}\tilde{\mathcal{C}_2}^T\sum_{j=1}^N Q_s^j\Gamma(u,v). \tag{3.7}$$

We then substitute Eqs. (2.13), (3.3), (3.4), and (3.5) into Eq. (1.1), resulting in the following expression.

$$\Gamma^T(u,v)Q \simeq \Gamma^T(u,v)Q + \Gamma^T(u,v)\Lambda\tilde{\mathcal{C}_1}^T Q_o \Gamma(u,v) + 2\Gamma^T(u,v)\dot{\Lambda}\tilde{\mathcal{C}_2}^T \sum_{j=1}^{N} Q_s^j \Gamma(u,v). \tag{3.8}$$

By replacing $\simeq$ with $=$ in (3.6), we obtain the following equation:

$$Q \simeq Q + \left( \Lambda\tilde{\mathcal{C}_1}^T Q_o + 2\dot{\Lambda}\tilde{\mathcal{C}_2}^T \sum_{j=1}^{N} Q_s^j \right) \Gamma(u,v). \tag{3.9}$$

By applying Eq. (3.7) at the Newton-Cotes points, we derive the following:

$$u_\alpha = \frac{2\alpha - 1}{2(m_1+1)}, \quad v_\beta = \frac{2\beta - 1}{2(m_2+1)},$$

where $\alpha = 1, 2, \ldots, (m_1+1)$ and $\beta = 1, 2, \ldots, (m_2+1)$, a system of $(m_1+1)(m_2+1)$ linear equations with $(m_1+1)(m_2+1)$ unknowns is generated. This system can be solved using established techniques, such as direct or iterative methods.

## 4. Error analysis

This section studies the error analysis for the method introduced earlier. The 2-norm is used throughout, defined for any continuous function $\psi \in C[\alpha,\beta]^n$ as follows:

$$\|\psi\|_2 = \left[ \underbrace{\int_\alpha^\beta \int_\alpha^\beta \cdots \int_\alpha^\beta}_{m \text{ times}} |\psi(u_1, u_2, \ldots, u_m)|^2 \, du_1 \, du_2 \cdots du_m \right]^{1/2}.$$

Now, we list the following theorems to determine the standard convergence rate of the proposed method.

**Theorem 2 ( [27])** Consider $\psi : [0,1]^n \to \mathbb{R}$ as a continuous function. The multivariate Bernstein polynomials $(\mathbb{B}r_{m_1,m_2,\ldots,m_m}\psi)$ will uniformly converge to $\psi$ as $m_1, m_2, \ldots, m_m$ approach infinity. Consequently, we have:

$$\begin{aligned}(\mathbb{B}r_{m_1,m_2,\ldots,m_m}\psi)(v_1,v_2,\ldots,v_m) = &\sum_{0\le\omega_\alpha\le m_\alpha,\ \alpha=1,2,\ldots,m} \psi\left(\frac{\omega_1}{m_1},\ldots,\frac{\omega_m}{m_m}\right) \\ &\times \prod_{\alpha=1}^{n} \binom{m_\alpha}{\omega_\alpha} v_\alpha^{\omega_\alpha}(1-v_\alpha)^{m_\alpha-\omega_\alpha}.\end{aligned} \tag{4.1}$$

**Theorem 3 ( [27])** Let $\psi : [0,1]^n \to \mathbb{R}$ be a continuous function. If

$$\|\psi(U) - \psi(V)\|_2 \le M\|U - V\|_2,$$

on $[0,1]^n$, then the inequality

$$\|(\mathbb{B}r_{m_1,m_2,\ldots,m_m}\psi)(U) - \psi(U)\|_2 < \frac{n}{2}\left(\sum_{\alpha=1}^{n}\frac{1}{m_\alpha}\right)^2, \tag{4.2}$$

holds.

**Theorem 4 ( [25,31])** For any continuous function $\psi(v)$ with modulus of continuity $\Theta(\psi,\varpi)$, the Bernstein polynomials $(\mathbb{B}r_m\psi)$ satisfy

$$|(\mathbb{B}r_m\psi)(v) - \psi(v)| \le \frac{5}{4}\Theta(\psi; n^{-1/2}), \tag{4.3}$$

where

$$\Theta(\psi;\varpi) = \sup_{|v_1-v_2|\le\varpi} |\psi(v_1) - \psi(v_2)|, \quad v_1, v_2 \in [0,1]. \tag{4.4}$$

**Theorem 5 ( [28])** Consider $H(V)$ as a continuous function including a modulus of continuity $\Theta(H, \varpi)$, where $V$ belongs to the interval $[0,1]^n$. Additionally, we have:

$$\Theta(H;\varpi) = \sup_{\|V_1 - V_2\|_2 \leq \varpi} |H(V_1) - H(V_2)|, \quad V_1, V_2 \in [0,1]^n. \tag{4.5}$$

Then, we obtain

$$|(\mathbb{B}r_m H)(V) - H(V)| \leq \frac{5}{4}\Theta(H; n^{-1/2}), \tag{4.6}$$

where $m = \sum_{\alpha=1}^{n} m_\alpha$.

**Theorem 6** Assume that $h(u,v)$ is the exact solution of Eq. (1.1) and $\hat{h}_m(u,v)$ is its approximation using Bernstein polynomials (BPs). Let $\hat{q}_m(u,v)$, $\hat{K_1}_m(u,v,\eta,\mu)$, and $\hat{K_2}_m(u,v,\eta,\mu)$ represent the BP approximations of the functions $q(u,v)$, $K_1(u,v,\eta,\mu)$, and $K_2(u,v,\eta,\mu)$, respectively. Additionally, assume that:

1. $\|h\|_2 \leq \Delta, \quad (u,v) \in [0,1]^2$,
2. $\|K_1\|_2 \leq \nabla_1, \quad (u,v,\eta,\mu) \in [0,1]^4$,
3. $\|K_2\|_2 \leq \nabla_2, \quad (u,v,\eta,\mu) \in [0,1]^4$,
4. $q$, $K_1$, and $K_2$ are continuous functions that satisfy the Lipschitz condition,
5. $m_1 = m_2 = m$,
6. $\left[\nabla_1 + \mathcal{O}\left(\frac{1}{m}\right) + \sum_{j=1}^{N} \mathcal{B}_j^2(1)\left(\nabla_2 + \mathcal{O}\left(\frac{1}{m}\right)\right)\right] < 1$,

Then, for every $(u,v) \in [0,1]^2$, we have

$$\|h - \hat{h}_m\|_2 = \mathcal{O}\left(\frac{1}{m}\right). \tag{4.7}$$

**Proof:** We can write

$$\begin{aligned} h(u,v) - \hat{h}_m(u,v) &= q(u,v) - \hat{q}_m(u,v) \\ &+ \int_0^1 \int_0^1 \left(K_1(u,v,\eta,\mu)h(\eta,\mu) - \hat{K_1}_m(u,v,\eta,\mu)\hat{h}_m(\eta,\mu)\right) d\eta\, d\mu \\ &+ \sum_{j=1}^{n} \int_0^1 \int_0^1 \left(K_2(u,v,\eta,\mu)h(\eta,\mu) - \hat{K_2}_m(u,v,\eta,\mu)\hat{h}_m(\eta,\mu)\right) d\mathcal{B}_j(\eta)\, d\mathcal{B}_j(\mu). \end{aligned}$$

Applying the mean value theorem for 2D integrals, for every $(u,v) \in [0,1]^2$ and $(u,v,\eta,\mu) \in [0,1]^4$, it follows that:

$$\|h - \hat{h}_m\|_2 \leq \|q - \hat{q}_m\|_2 + \|K_1 h - \hat{K_1}_m \hat{h}_m\|_2 + \sum_{j=1}^{N} \mathcal{B}_j^2(1)\|K_2 h - \hat{K_2}_m \hat{h}_m\|_2. \tag{4.8}$$

Based on the Hypotheses 1 and 2 along with Theorem 3, yields

$$\begin{aligned} \|K_1 h - \hat{K_1}_m \hat{h}_m\|_2 &\leq \|K_1\|_2 \|h - \hat{h}_m\|_2 + \|K_1 - \hat{K_1}_m\|_2 \left(\|h - \hat{h}_m\|_2 + \Delta\right) \\ &\leq \nabla_1 \|h - \hat{h}_m\|_2 + \mathcal{O}\left(\frac{1}{m}\right)\left(\|h - \hat{h}_m\|_2 + \Delta\right) \\ &= \left(\nabla_1 + \mathcal{O}\left(\frac{1}{m}\right)\right)\|h - \hat{h}_m\|_2 + \mathcal{O}\left(\frac{1}{m}\right)\Delta. \end{aligned}$$

Similarly, by using Hypotheses 1 and 3 along with Theorem 3, we can write

$$\|K_2 h - \hat{K}_{2m}\hat{h}_m\|_2 \leq \left(\nabla_2 + \mathcal{O}\left(\frac{1}{m}\right)\right)\|h - \hat{h}_m\|_2 + \mathcal{O}\left(\frac{1}{m}\right)\Delta. \tag{4.9}$$

By substituting (3.9) and (4.1) in (3.8) and Theorem 3, we get

$$\begin{aligned}\|h - \hat{h}_m\|_2 \leq O\left(\frac{1}{m}\right) &+ \left[\left(\nabla_1 + \mathcal{O}\left(\frac{1}{m}\right)\right)\|h - \hat{h}_m\|_2 + \mathcal{O}\left(\frac{1}{m}\right)\Delta\right] \\ &+ \sum_{j=1}^{N}\mathcal{B}_j^2(1)\left[\left(\nabla_2 + \mathcal{O}\left(\frac{1}{m}\right)\right)\|h - \hat{h}_m\|_2 + \mathcal{O}\left(\frac{1}{m}\right)\Delta\right].\end{aligned}$$

By taking the supremum, we obtain the following inequality:

$$\begin{aligned}\|h - \hat{h}_m\|_2 \leq O\left(\frac{1}{m}\right) &+ \left[\left(\nabla_1 + \mathcal{O}\left(\frac{1}{m}\right)\right)\sup_{\eta\leq u,\mu\leq v}\|h(\eta,\mu) - \hat{h}_m(\eta,\mu)\|_2 + \mathcal{O}\left(\frac{1}{m}\right)\Delta\right] \\ &+ \sum_{j=1}^{N}\mathcal{B}_j^2(1)\left[\left(\nabla_2 + \mathcal{O}\left(\frac{1}{m}\right)\right)\sup_{\eta\leq u,\mu\leq v}\|h(\eta,\mu) - \hat{h}_m(\eta,\mu)\|_2 + \mathcal{O}\left(\frac{1}{m}\right)\Delta\right].\end{aligned}$$

This implies that

$$\|h - \hat{h}_m\|_2 \leq \frac{\mathcal{O}\left(\frac{1}{m}\right)\left[1 + \Delta + \sum_{j=1}^{N}\mathcal{B}_j^2(1)\Delta\right]}{1 - \left[\nabla_1 + \mathcal{O}\left(\frac{1}{m}\right) + \sum_{j=1}^{N}\mathcal{B}_j^2(1)\left(\nabla_2 + \mathcal{O}\left(\frac{1}{m}\right)\right)\right]},$$

and finally, applying Hypothesis 6, we obtain:

$$\|h - \hat{h}_m\|_2 = \mathcal{O}\left(\frac{1}{m}\right).$$

□

**Theorem 7** Let us assume that $h(u,v)$ denotes the exact solution to Eq. (1.1) and that $\hat{h}_m(u,v)$ represents the BP approximation derived from Eq. (3.7). Additionally, let $\hat{q}_m(u,v)$, $\hat{K}_{1m}(u,v,\eta,\mu)$, and $\hat{K}_{2m}(u,v,\eta,\mu)$ be the Bernstein polynomial approximations of the functions $q(u,v)$, $K_1(u,v,\eta,\mu)$, and $K_2(u,v,\eta,\mu)$, respectively. Moreover, consider $\Theta(K,\varpi)$ as the modulus of continuity for a given continuous function $K(V)$, where $V \in [0,1]^n$. Finally, consider the following conditions:

1. $\|h\|_2 \leq \Delta, \quad (u,v) \in [0,1]^2,$
2. $\|K_1\|_2 \leq \nabla_1, \quad (u,v,\eta,\mu) \in [0,1]^4,$
3. $\|K_2\|_2 \leq \nabla_2, \quad (u,v,\eta,\mu) \in [0,1]^4,$
4. $m_1 = m_2 = m,$
5. $\left[\nabla_1 + \frac{5}{4}\Theta\left(K_1;(4n)^{-1/2}\right) + \sum_{j=1}^{N}\mathcal{B}_j^2(1)\left(\nabla_2 + \frac{5}{4}\Theta\left(K_2;(4n)^{-1/2}\right)\right)\right] < 1,$

Then for every $(u,v) \in [0,1]^2$, we have

$$\|h - \hat{h}_m\|_2 \leq \frac{5\mathcal{C}_0}{4}\left[\Theta\left(q;(2n)^{-1/2}\right) + \Theta\left(K_1;(4n)^{-1/2}\right)\Delta + \Theta\left(K_2;(4n)^{-1/2}\right)\Delta\sum_{j=1}^{N}\mathcal{B}_j^2(1)\right], \tag{4.10}$$

where $\mathcal{C}_0$ represents a real constant.

**Proof:** Considering inequality (3.8) in conjunction with Hypotheses 1 and 2, as well as Theorems 4 and 5, we can write as follows:

$$\begin{aligned}\|K_1h - \hat{K}_{1m}\hat{h}_m\|_2 &\leq \|K_1\|_2\|h-\hat{h}_m\|_2 + \|K_1-\hat{K}_{1m}\|_2\left(\|h-\hat{h}_m\|_2+\Delta\right)\\ &\leq \nabla_1\|h-\hat{h}_m\|_2 + \frac{5}{4}\Theta\left(K_1;(4n)^{-1/2}\right)\left(\|h-\hat{h}_m\|_2+\Delta\right)\\ &\leq \left(\nabla_1+\frac{5}{4}\Theta\left(K_1;(4n)^{-1/2}\right)\right)\|h-\hat{h}_m\|_2 + \frac{5}{4}\Theta\left(K_1;(4n)^{-1/2}\right)\Delta.\end{aligned}$$

In a similar manner, utilizing Hypotheses 1 and 3, along with Theorems 4 and 5, we obtain

$$\begin{aligned}\|K_2h - \hat{K}_{2m}\hat{h}_m\|_2 &\leq \|K_2\|_2\|h-\hat{h}_m\|_2 + \|K_2-\hat{K}_{2m}\|_2\left(\|h-\hat{h}_m\|_2+\Delta\right)\\ &\leq \left(\nabla_2+\frac{5}{4}\Theta\left(K_2;(4n)^{-1/2}\right)\right)\|h-\hat{h}_m\|_2 + \frac{5}{4}\Theta\left(K_2;(4n)^{-1/2}\right)\Delta. \qquad (4.11)\end{aligned}$$

Then, substituting (4.2) and (4.3) into (3.8) and using Theorem 5, we have

$$\begin{aligned}\|h-\hat{h}_m\|_2 \leq{}& \frac{5}{4}\Theta\left(q;(2n)^{-1/2}\right)\\ &+\left[\left(\nabla_1+\frac{5}{4}\Theta\left(K_1;(4n)^{-1/2}\right)\right)\|h-\hat{h}_m\|_2 + \frac{5}{4}\Theta\left(K_1;(4n)^{-1/2}\right)\Delta\right]\\ &+\sum_{j=1}^{N}\mathcal{B}_j^2(1)\left[\left(\nabla_2+\frac{5}{4}\Theta\left(K_2;(4n)^{-1/2}\right)\right)\|h-\hat{h}_m\|_2 + \frac{5}{4}\Theta\left(K_2;(4n)^{-1/2}\right)\Delta\right].\end{aligned}$$

Taking the supremum results in the following inequality:

$$\begin{aligned}\|h-\hat{h}_m\|_2 \leq{}& \frac{5}{4}\Theta\left(q;(2n)^{-1/2}\right)\\ &+\left[\left(\nabla_1+\frac{5}{4}\Theta\left(K_1;(4n)^{-1/2}\right)\right)\sup_{\eta\leq u,\mu\leq v}\|h(\eta,\mu)-\hat{h}_m(\eta,\mu)\|_2 + \frac{5}{4}\Theta\left(K_1;(4n)^{-1/2}\right)\Delta\right]\\ &+\sum_{j=1}^{N}\mathcal{B}_j^2(1)\left[\left(\nabla_2+\frac{5}{4}\Theta\left(K_2;(4n)^{-1/2}\right)\right)\sup_{\eta\leq u,\mu\leq v}\|h(\eta,\mu)-\hat{h}_m(\eta,\mu)\|_2 + \frac{5}{4}\Theta\left(K_2;(4n)^{-1/2}\right)\Delta\right].\end{aligned}$$

This implies that

$$\|h-\hat{h}_m\|_2 \leq \frac{\frac{5}{4}\Theta\left(q;(2n)^{-1/2}\right)+\frac{5}{4}\Theta\left(K_1;(4n)^{-1/2}\right)\Delta+\frac{5}{4}\sum_{j=1}^{N}\mathcal{B}_j^2(1)\Theta\left(K_2;(4n)^{-1/2}\right)\Delta}{1-\left[\nabla_1+\frac{5}{4}\Theta\left(K_1;(4n)^{-1/2}\right)+\sum_{j=1}^{N}\mathcal{B}_j^2(1)\left(\nabla_2+\frac{5}{4}\Theta\left(K_2;(4n)^{-1/2}\right)\right)\right]}.$$

Therefore, by Hypothesis 5, we can obtain

$$\|h-\hat{h}_m\|_2 \leq \frac{5\mathcal{C}_0}{4}\left[\Theta\left(q;(2n)^{-1/2}\right)+\Theta\left(K_1;(4n)^{-1/2}\right)\Delta+\Theta\left(K_2;(4n)^{-1/2}\right)\Delta\sum_{j=1}^{N}\mathcal{B}_j^2(1)\right],$$

where $\mathcal{C}_0$ represents a real constant. □

## 5. Numerical examples

This section presents two numerical examples to demonstrate the effectiveness of the proposed method. For these examples, the error average, the solution average, 95% confidence interval, and confidence interval length at selected points $(u, v)$ for various values of $n$ are denoted by $\bar{e}(u, v)$, $\bar{h}(u, v)$, $CI$, and $CLI$, respectively, in the following tables. The results obtained using this method are compared with those from HWFs [16] and BPFs [17,18] and are presented in Tables 2 and 4. For simplicity, we set $m_1 = m_2 = m$. All computations were carried out using MAPLE 15 on a Pentium IV processor (2.80 GHz) with 4 GB of RAM.

**Example 1** Consider the following 2D linear stochastic Fredholm integral equation with multiple noise of the second kind:

$$h(u,v) = q(u,v) + \int_0^1 \int_0^1 \mu\sqrt{uv}\sin(\eta)h(\eta,\mu)\,d\eta\,d\mu + \sum_{j=1}^{3}\int_0^1 \int_0^1 \eta\mu\cos(uv)h(\eta,\mu)\,d\mathcal{B}_j(\eta)\,d\mathcal{B}_j(\mu),$$

where

$$\begin{aligned} q(u,v) = (uv)e^{\sum_{j=1}^{3}\mathcal{B}_j(u)+\mathcal{B}_j(v)} &- \int_0^1 \int_0^1 \mu^2\eta\sqrt{uv}\sin(\eta)e^{\sum_{j=1}^{3}\mathcal{B}_j(\eta)+\mathcal{B}_j(\mu)}\,d\eta\,d\mu \\ &- \cos(uv)\left(e^{\sum_{j=1}^{3}\mathcal{B}_j(1)} - \int_0^1 e^{\sum_{j=1}^{3}\mathcal{B}_j(\mu)}\left(2\mu + \frac{\mu^2}{2}\right)d\mu\right)^2. \end{aligned}$$

The exact solution to the above example can be determined as

$$h(u,v) = (uv)e^{\sum_{j=1}^{3}\mathcal{B}_j(u)+\mathcal{B}_j(v)}.$$

**Example 2** Consider the following 2D-linear stochastic Fredholm integral equation with multiple noise of the second kind:

$$h(u,v) = q(u,v) + \int_0^1 \int_0^1 (uv\eta\mu)h(\eta,\mu)\,d\eta\,d\mu + \sum_{j=1}^{3}\int_0^1 \int_0^1 (u+v+\eta+\mu)h(\eta,\mu)\,d\mathcal{B}_j(\eta)\,d\mathcal{B}_j(\mu),$$

where

$$\begin{aligned} q(u,v) = u + v - \frac{uv}{3} &- 2(u+v)\sum_{j=1}^{3}\mathcal{B}_j(1)\left(\mathcal{B}_j(1) - \int_0^1 \mathcal{B}_j(\eta)\,d\eta\right) \\ &- 2\sum_{j=1}^{3}\mathcal{B}_j(1)\left(\mathcal{B}_j(1) - 2\int_0^1 \mathcal{B}_j(\eta)\,d\eta\right) - 2\left(\mathcal{B}_j(1) - \int_0^1 \mathcal{B}_j(\eta)\,d\eta\right)^2. \end{aligned}$$

The exact solution for the above example is given by

$$h(u,v) = u + v.$$

Table 1: The mean solution $\bar{h}(u,v)$, error mean $\bar{e}(u,v)$, 95% confidence interval $(CI)$, and the confidence interval length $(CLI)$ for Example 1.

| $(u,v)$ | $m$ | $\bar{g}(u,v)$ | $\bar{e}(u,v)$ | CI | LCI |
|---|---|---|---|---|---|
| $(0.1,0.3)$ | 2 | $-0.374176$ | 0.381898 | $(-0.8356,0.08725)$ | 0.92285 |
| | 4 | $-0.149460$ | 0.032923 | $(-0.3068,0.20796)$ | 0.51476 |
| | 6 | $-0.122804$ | 0.002616 | $(-0.1371,-0.0004)$ | 0.13639 |
| $(0.4,0.4)$ | 2 | $-0.009997$ | 0.294952 | $(-0.3566,0.03366)$ | 0.69326 |
| | 4 | $-0.202087$ | 0.010516 | $(-0.3860,-0.0181)$ | 0.36787 |
| | 6 | $-0.161661$ | 0.007575 | $(-0.1717,0.00039)$ | 0.17209 |
| $(0.8,0.6)$ | 2 | $-0.109514$ | 0.197593 | $(-0.3054,0.08642)$ | 0.39188 |
| | 4 | 0.0075860 | 0.090158 | $(-0.0196,0.23480)$ | 0.25440 |
| | 6 | 0.0714780 | 0.005641 | $(-0.0622,0.10518)$ | 0.16738 |

Table 2: A comparative analysis of 95% confidence interval (CI), the error mean $\bar{e}(u,v)$, and the confidence interval length $(CLI)$ for the BPs method versus the HWFs and BPFs methods, for Example 2.

| $(u,v)$ | $m$ | $Method$ | $\bar{e}(u,v)$ | $CI$ | $LCI$ |
|---|---|---|---|---|---|
| $(0.125,0.625)$ | 2 | HWFs | 0.644204 | $(-0.3354,1.20925)$ | 1.54469 |
| | | BPFs | 0.430623 | $(-0.3471,0.81229)$ | 1.15940 |
| | | BPs | 0.083247 | $(-0.2655,0.11632)$ | 0.38190 |
| $(0.625,0.375)$ | 2 | HWFs | 0.836627 | $(-0.2597,1.63020)$ | 1.96564 |
| | | BPFs | 0.406720 | $(-0.3471,0.81229)$ | 1.15940 |
| | | BPs | 0.004444 | $(-0.1952,0.20255)$ | 0.39783 |
| $(0.187,0.687)$ | 4 | HWFs | 0.204906 | $(0.24458,0.65826)$ | 0.41368 |
| | | BPFs | 0.573738 | $(-0.8666,0.72258)$ | 1.58918 |
| | | BPs | 0.007350 | $(-0.0168,0.13136)$ | 0.14816 |
| $(0.562,0.562)$ | 4 | HWFs | 0.609751 | $(0.14182,1.50142)$ | 1.35960 |
| | | BPFs | 0.530567 | $(-0.6820,0.62439)$ | 1.30639 |
| | | BPs | 0.043660 | $(-0.0107,0.24812)$ | 0.25882 |

Table 3: The mean solution $\bar{h}(u,v)$, error mean $\bar{e}(u,v)$, 95% confidence interval $(CI)$, and the confidence interval length $(LCI)$ for Example 2.

| $(u,v)$ | $m$ | $\bar{g}(u,v)$ | $\bar{e}(u,v)$ | $CI$ | $LCI$ |
|---|---|---|---|---|---|
| $(0.1,0.3)$ | 2 | 1.088080 | 0.276765 | $(0.29598,1.18017)$ | 0.88419 |
| | 4 | 0.863974 | 0.063974 | $(0.53232,1.19563)$ | 0.66330 |
| | 6 | 0.515669 | 0.015669 | $(0.43306,0.76440)$ | 0.33134 |
| $(0.4,0.4)$ | 2 | 0.396699 | 0.187558 | $(0.26779,0.86118)$ | 0.59339 |
| | 4 | 0.540188 | 0.032910 | $(0.30865,0.88902)$ | 0.58037 |
| | 6 | 0.564434 | 0.005566 | $(0.30330,0.52556)$ | 0.22226 |
| $(0.9,0.2)$ | 2 | 0.399475 | 0.148783 | $(0.18052,0.77947)$ | 0.59895 |
| | 4 | 0.465394 | 0.034606 | $(0.33004,0.76083)$ | 0.43079 |
| | 6 | 0.809044 | 0.001126 | $(0.38310,0.50119)$ | 0.11809 |

Table 4: A comparative analysis of 95% confidence interval, the error mean $\bar{e}(u,v)$, and confidence interval length for the BPs method versus the HWFs and BPFs methods, for Example 2.

| $(u,v)$ | $m$ | Method | $\bar{e}(u,v)$ | CI | LCI |
|---|---|---|---|---|---|
| $(0.125, 0.625)$ | 2 | HWFs | 0.809726 | $(-1.0731, 0.95370)$ | 2.02686 |
| | | BPFs | 0.437228 | $(0.09462, 1.27983)$ | 1.18520 |
| | | BPs | 0.008105 | $(0.71651, 0.74727)$ | 0.03075 |
| $(0.375, 0.375)$ | 2 | HWFs | 0.520358 | $(-0.2003, 1.10245)$ | 1.30277 |
| | | BPFs | 0.010698 | $(-0.8132, 0.69183)$ | 1.50506 |
| | | BPs | 0.008634 | $(0.69593, 0.72680)$ | 0.03086 |
| $(0.187, 0.687)$ | 4 | HWFs | 0.527728 | $(-0.3117, 1.00630)$ | 1.31806 |
| | | BPFs | 0.580585 | $(-0.1626, 0.75148)$ | 0.91412 |
| | | BPs | 0.098661 | $(0.50983, 0.54064)$ | 0.03081 |
| $(0.937, 0.312)$ | 4 | HWFs | 0.809701 | $(-0.3169, 1.50530)$ | 1.82224 |
| | | BPFs | 0.771418 | $(-0.3123, 1.26947)$ | 1.58177 |
| | | BPs | 0.048950 | $(0.18460, 0.48050)$ | 0.29590 |

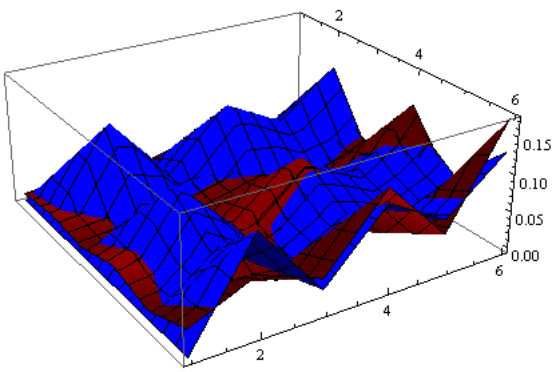


Figure 1: Exact and numerical solution for Example 1 ($n = 5$)

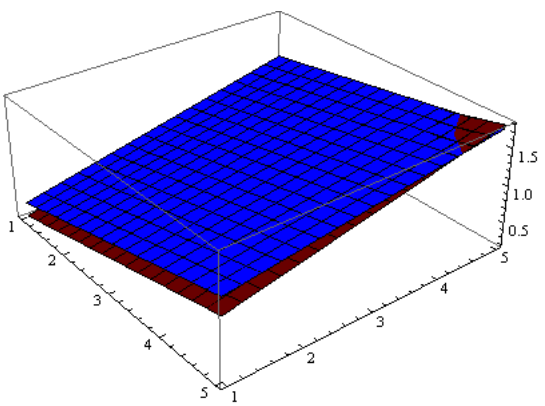


Figure 2: Exact and numerical solutions for Example 2 ($n = 5$)

Tables 1 and 3 demonstrate that, in the proposed method, both the confidence interval length and the error mean decrease as $n$ increases. This trend clearly reflects the convergence behavior of the algorithm, indicating that larger values of $n$ enhance the approximation accuracy and lead to more reliable statistical estimates. In addition, the reduction in confidence interval length with increasing $n$ implies higher

precision in the computed results, which is a desirable feature in numerical simulations of stochastic models. Moreover, Tables 2 and 4 show that the BPs method consistently yields a shorter confidence interval and a lower error mean compared to other competing methods considered in this study. This superiority is observed across different problem settings, confirming the robustness and efficiency of the BPs approach in handling multi-noise stochastic Fredholm integral equations. To further illustrate the performance of the proposed method, three-dimensional plots of the exact and approximate solutions for Examples 1 and 2, corresponding to the arbitrary positive integer $n = 5$, are presented in Figures 1 and 2. In these plots, the approximate surfaces generated by the proposed scheme exhibit an excellent visual agreement with the exact solutions, thereby reinforcing the quantitative results summarized in the tables. The smoothness and closeness of the approximate surfaces to the exact ones also highlight the capability of the method to capture the underlying behavior of the solutions with high fidelity.

## 6. Conclusion

This paper implemented a novel approach based on two-dimensional Bernstein polynomials (2DBPs) and their operational integration matrices for approximating the solution of the 2D-LMN-SFIE (1.1). Error analysis and numerical experiments demonstrated the accuracy of the proposed method. A key advantage of this approach was its lower computational cost in setting up the system of equations, as it eliminated the need for integration. Numerical results indicated that the Bernstein approximation method was highly effective, straightforward, and reliable for solving two-dimensional linear multi-noise stochastic Fredholm integral equations of the second kind with high accuracy. The numerical experiments confirmed that the typical convergence rate of the method was $\mathcal{O}\left(\frac{1}{m}\right)$. Furthermore, the method could be iteratively refined by increasing $n$ until the desired level of accuracy was achieved. Finally, this method could be extended and applied to two-dimensional linear multi-noise stochastic Volterra–Fredholm integral equations of both the first and second kinds.

## Availability of data and materials

No data was used in the research presented in this article.

## Competing interests

The authors declare that there are no conflicts of interest.

## References

1. P. P. Paikaray, S. Beuria, and N. Ch. Parida, Numerical approximation of $p$-dimensional stochastic Volterra integral equation using Walsh function, *Journal of Mathematics and Computer Science*, vol. 31, no. 4, pp. 448–460, (2023).

2. P. P. Paikaray, N. C. Parida, S. Beuria, O. Nikan, Numerical approximation of nonlinear stochastic Volterra integral equation based on Walsh function, SeMA, vol. 81, pp. 665–678, (2024).

3. H. H. G. Hashem and H. O. Alrashidi, Characteristics of solutions of nonlinear neutral integro-differential equation via Chandrasekhar integral, *Journal of Mathematics and Computer Science*, vol. 24, no. 2, pp. 173–185, (2022).

4. S. Kriket and A. Boudeliou, A class of nonlinear delay integral inequalities for two-variable functions and their applications in Volterra integral equations, *Journal of Mathematics and Computer Science*, vol. 32, no. 1, pp. 1–12, (2024).

5. A. Golbabai, O. Nikan, and J. R. Tousi, Note on using radial basis functions method for solving nonlinear integral equations, *Communications in Numerical Analysis*, vol. 2, pp. 81–91, (2016).

6. M. Luo, W. Qiu, O. Nikan, and Z. Avazzadeh, Second-order accurate, robust and efficient ADI Galerkin technique for the three-dimensional nonlocal heat model arising in viscoelasticity, *Applied Mathematics and Computation*, vol. 440, 127655, (2023).

7. Q. Huang, O. Nikan, and Z. Avazzadeh, Numerical analysis of alternating direction implicit orthogonal spline collocation scheme for the hyperbolic integrodifferential equation with a weakly singular kernel, *Mathematics*, vol. 10, no. 18, p. 3390, (2022).

8. O. Nikan, J. T. Machado, A. Golbabai, and J. Rashidinia, Numerical evaluation of the fractional Klein–Kramers model arising in molecular dynamics, *Journal of Computational Physics*, vol. 428, p. 109983, (2021).

9. Y. E. Aghdam, H. Mesgarani, M. Javidi, and O. Nikan, A computational approach for the space-time fractional advection–diffusion equation arising in contaminant transport through porous media, *Engineering Computations*, vol. 37, no. 4, pp. 3615–3627, (2021).

10. O. Nikan, A. Golbabai, J. T. Machado, and T. Nikazad, Numerical solution of the fractional Rayleigh–Stokes model arising in a heated generalized second-grade fluid, *Engineering Computations*, vol. 37, no. 3, pp. 1751–1764, (2021).

11. O. Nikan, J. A. Tenreiro Machado, A. Golbabai, and T. Nikazad, Numerical investigation of the nonlinear modified anomalous diffusion process, *Nonlinear Dynamics*, vol. 97, no. 4, pp. 2757–2775, (2019).

12. O. Nikan, J. Rashidinia, and H. Jafari, Numerically pricing American and European options using a time fractional Black–Scholes model in financial decision-making, *Alexandria Engineering Journal*, vol. 112, pp. 235–245, (2025).

13. O. Nikan, J. Rashidinia, and H. Jafari, An improved local radial basis function method for pricing options under the time-fractional Black–Scholes model, *Journal of Computational Science*, 102610, (2025).

14. W. Qiu, O. Nikan, and Z. Avazzadeh, Numerical investigation of generalized tempered-type integrodifferential equations with respect to another function, *Fractional Calculus and Applied Analysis*, vol. 26, no. 6, pp. 2580–2601, (2023).

15. H. Mesgarani, J. Rashidinia, Y. E. Aghdam, and O. Nikan, Numerical treatment of the space fractional advection–dispersion model arising in groundwater hydrology, *Computational and Applied Mathematics*, vol. 40, no. 1, pp. 1–17, (2021).

16. M. Fallahpour, M. Khodabin, and K. Maleknejad, Approximate solution of two-dimensional linear stochastic Fredholm integral equation by applying the Haar wavelet, *International Journal of Mathematical Modelling and Computations*, vol. 5, no. 4, pp. 361–372, (2015).

17. M. Fallahpour, M. Khodabin, and K. Maleknejad, Approximate solution of two-dimensional linear stochastic Volterra–Fredholm integral equation via two-dimensional Block-pulse functions, *International Journal of Industrial Mathematics*, vol. 8, no. 4, Article ID IJIM-00774, (2016).

18. M. Fallahpour, M. Khodabin, and K. Maleknejad, Theoretical error analysis and validation in the numerical solution of two-dimensional linear stochastic Volterra–Fredholm integral equation by applying block-pulse functions, *Cogent Mathematics*, vol. 4, 1296750, (2017).

19. E. Solhi, F. Mirzaee, and S. Naserifar, Approximate solution of two-dimensional linear and nonlinear stochastic Itô–Volterra integral equations via meshless scheme, *Mathematics and Computers in Simulation*, vol. 207, pp. 369–387, (2023).

20. P. K. Singh and S. Saha Ray, A novel operational matrix method based on Genocchi polynomials for solving n-dimensional stochastic Itô–Volterra integral equation, *Mathematical Sciences*, vol. 18, pp. 305–315, (2024).

21. I. Boukhelkhal and R. Zeghdane, Lagrange interpolation polynomials for solving nonlinear stochastic integral equations, *Numerical Algorithms*, vol. 96, pp. 583–618, (2024).

22. A. Z. Amin, A. K. Amin, M. A. Abdelkawy, A. A. Alluhaybi, and I. Hashim, Spectral technique with convergence analysis for solving one and two-dimensional mixed Volterra–Fredholm integral equation, *PLoS One*, vol. 18, no. 5, e0283746, (2023).

23. J. Mi and J. Huang, Collocation method for solving two-dimensional nonlinear Volterra–Fredholm integral equations with convergence analysis, *Journal of Computational and Applied Mathematics*, vol. 428, 115188, (2023).

24. H. H. Kuo, *Introduction to Stochastic Integration*, Springer Science+Business Media, Inc., (2006).

25. G. G. Lorentz, *Bernstein Polynomials*, Chelsea Publishing Company, New York, (1986).

26. T. J. Rivlin, *An Introduction to the Approximation of Functions*, Dover Publications, New York, (1969).

27. C. Heitzinger, *Simulation and Inverse Modeling of Semiconductor Manufacturing Processes*, TU Wien Bibliothek, Wien, Austria, (2002). Available: http://www.iue.tuwien.ac.at/phd/heitzinger/node130.html

28. A. Pallini, Bernstein-type approximations of smooth functions, *Statistica*, vol. 65, no. 2, pp. 169–191, (2005).

29. F. H. Shekarabi, K. Maleknejad, and R. Ezzati, Application of two-dimensional Bernstein polynomials for solving mixed Volterra–Fredholm integral equations, *African Mathematics*, vol. 26, no. 7, pp. 1237–1251, (2015).

30. M. Asgari, E. Hashemizadeh, M. Khodabin, and K. Maleknejad, Numerical solution of nonlinear stochastic integral equation by stochastic operational matrix based on Bernstein polynomials, *Bulletin of the Mathematical Society of the Sciences Mathematical Roumanie*, Tome 57(105), no. 1, pp. 3–12, (2014).

31. T. Popoviciu, Sur l'approximation des fonctions convexes d'ordre supérieur, *Mutlzemntica (Cluj)*, vol. 10, pp. 49–54, (1935).

*Murtadha Ali Shabeeb,*

*Department of Mathematics, College of Education, Misan University,*

*Misan, 62001, Iraq.*

*E-mail address:* murtadha.alallaq@gmail.com

*and*

*Mohsen Fallahpour and Reza Ezzati,*
*Department of Mathematics, Karaj Branch, Islamic Azad University,*
*Karaj 31499-68111, Iran.*
*E-mail address:* m.fallahpour@kiau.ac.ir
*E-mail address:* ezati@kiau.ac.ir

*and*

*Mohammad Navaz Rasoulizadeh*,*
*Department of Mathematics, Velayat University, Iranshahr, Iran*
*E-mail address:* mn.rasoulizadeh@velayat.ac.ir